

Preclinical studies of N₃-O-toluyfl-fluorouracil-loaded lipid-based nanosuspensions in H₂₂-bearing mice

Juan Zhang
Min Li
Zhihong Liu
Lili Wang
Yongjun Liu
Na Zhang

School of Pharmaceutical Science,
Shandong University, Ji'nan, People's
Republic of China

Purpose: N₃-O-toluyfl-fluorouracil (TFU) is a potential antitumor prodrug of 5-fluorouracil (5-FU), but its poor solubility has limited its use in clinic. This study aimed to improve the bioavailability of TFU by preparing TFU-loaded lipid-based nanosuspensions (TFU-LNS) and perform a preclinical evaluation.

Methods: TFU-LNS were prepared through high-pressure homogenization and were lyophilized afterwards. For in vitro test, the physicochemical properties and cytotoxicity against HegG2 cells were conducted. For in vivo evaluation, the pharmacokinetics, tissue distribution, and antitumor efficacy were investigated in H₂₂-bearing Kunming mice.

Results: TFU showed different degradability in four media; in particular, nearly all of it converted to an equimolar amount of 5-FU in blank plasma of Wistar rats. The lyophilized TFU-LNS had a mean particle size of 180.03±3.11 nm and zeta potential of -8.02±1.43 mV and showed no discernible changes after storage at 4°C for 3 months. In the in vivo antitumor study, the antitumor efficacy of TFU-LNS was consistent with that of 5-FU injection. Furthermore, TFU-LNS released a lower concentration of 5-FU in heart and kidney throughout the tissue distribution studies.

Conclusion: TFU-LNS exhibited convincing antitumor activity and easy scale-up opportunity, which suggests that TFU-LNS might be a promising drug delivery system for cancer therapy.

Keywords: 5-fluorouracil, high-pressure homogenization, cytotoxicity, cancer therapy

Introduction

5-fluorouracil (5-FU) has been widely used in the therapy for malignant tumors, including cancers of the stomach, liver, and intestine. Nevertheless, the half-life of 5-FU in plasma is too short (15–20 minutes), and the clinically effective dosage of 5-FU is very close to its toxic dosage during infusion, resulting in severe toxicities to gastrointestinal mucosa and bone marrow. N₃-O-toluyfl-fluorouracil (TFU) was synthesized as one of the effective prodrugs of 5-FU. As shown in Figure 1, TFU performs little pharmacological activity in vitro, while it can be metabolized into 5-FU in vivo by amidase activation. Due to the higher enzyme activity in the liver, TFU was expected to exhibit superior therapeutic effect in the treatment of hepatic carcinoma.¹ Strong anticancer activity of TFU has been demonstrated in animals.^{2–4} However, the clinical application of TFU is limited due to its poor solubility and low bioavailability. The solubility of TFU in phosphate-buffered saline ([PBS] pH 7.4) was merely 95 µg/mL, and its oil/water partition coefficient was 1.769,⁵ indicating that TFU belonged to class IV (poorly soluble, poorly permeable) in the Biopharmaceutics Classification System.⁶ Hence, a new formulation for improving the bioavailability and therapeutic index of TFU is desired.

Correspondence: Na Zhang
School of Pharmaceutical Science,
Shandong University, 44 Wenhua Xi
Road, Ji'nan 250012, People's Republic
of China
Tel +86 531 8838 2015
Fax +86 531 8838 2548
Email zhangnancy9@sdu.edu.cn

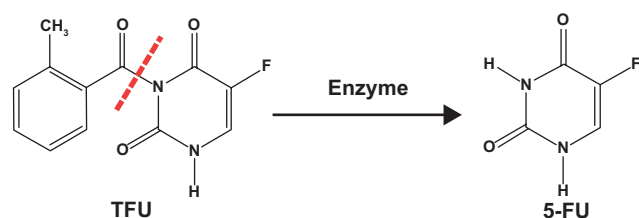


Figure 1 Scheme of metabolism from TFU to 5-FU.

Abbreviations: 5-FU, 5-fluorouracil; TFU, N₃-O-toluyfl-fluorouracil.

Recently, lipid-based nanocarriers have attracted increasing scientific and commercial attention as alternative carriers for delivering a new chemical entity with poor solubility or permeability.⁷ Based on the advantages of lipid-based materials and nanostructures, lipid-based nanocarriers present many favorable characteristics, such as: 1) improved drug dispersibility; 2) enhanced drug solubility; 3) enhanced drug transmembrane transport capability; 4) increased therapeutic efficacy by passive targeting; and 5) reduced toxicity with biocompatible or biodegradable components.^{8–11}

TFU has been previously encapsulated in several kinds of lipid-based formulations, such as liposomes^{1,12} and two types (cationic and anionic) of solid lipid nanoparticles.^{13–15} All three formulations enhanced the gastrointestinal absorption of TFU by oral administration, which was about twice that of TFU suspension. The three above-mentioned formulations could significantly enhance the bioavailability of TFU, but liposomes have suboptimal properties, such as high production cost, poor stability, and toxic solvent residue, while solid lipid nanoparticles have a low drug loading rate and are difficult to mass produce.

Nanosuspensions have emerged as a promising strategy for the efficient delivery of hydrophobic drugs by their large ratio of surface area to volume, and nanosuspensions can be defined as colloidal dispersions of nanosized drug particles (100–1,000 nm) that are stabilized by a suitable stabilizer.¹⁶ Nanosuspensions also exhibit many advantages, including: 1) high efficiency of drug loading; 2) easy scale-up for manufacture; 3) relatively low-cost preparation; and 4) applicability for various administration routes, such as oral, parenteral, ocular, and pulmonary delivery.^{11,17} A number of nanosuspensions have been used in clinic to combat cancer and other diseases, such as fenofibrate, aprepitant, sirolimus, megestrol, and paliperidone.^{18,19} Recently, lipid-based nanosuspensions (LNS), an innovative lipid-based nanocarrier, have been reported.²⁰ LNS are nanosuspensions with lipid materials as stabilizer, such as soya lecithin. High-pressure homogenization technology was used to prepare LNS, which provided a relatively easy scale-up

opportunity. In addition, only injectable phospholipids were used as the stabilizer, and no organic solvents were added during the preparation. Taking into account the advantages of lipid-based nanocarriers and nanosuspensions, LNS are expected to improve the low bioavailability of TFU and be more suited for industrial production.

Thus, the objective of the present study was to develop and characterize TFU-loaded LNS (TFU-LNS), so as to improve the bioavailability of TFU. In order to provide the basis for formulation design and rational use of TFU, the *in vitro* stability of TFU was evaluated after incubating with PBS (pH 7.4), simulated gastric fluid, simulated intestinal fluid, and the blank plasma of Wistar rats, respectively. Then, TFU-LNS were prepared by high-pressure homogenization technology and evaluated in terms of morphology, particle size, zeta potential, stability, and *in vitro* release properties. Furthermore, the *in vitro* cytotoxicity evaluation was performed in a human hepatoma cell line (HepG2). Finally, the *in vivo* antitumor efficacy, pharmacokinetics, and drug tissue distribution was evaluated in H₂₂-bearing Kunming mice. In particular, the release of 5-FU from TFU-LNS *in vivo* was detected in the studies of pharmacokinetics and biodistribution, and an equimolar amount of 5-FU injection was chosen for the control group.

Materials and methods

Materials

Injectable soya lecithin (phosphatidylcholine accounts for 95%, pH 5.0–7.0) was provided by Shanghai Taiwei Pharmaceutical Co., Ltd. (Shanghai, People's Republic of China). 5-FU injection was provided by Shanghai Xudonghaipu Pharmaceutical Co., Ltd. (Shanghai, People's Republic of China). All reagents for high-performance liquid chromatography (HPLC) analysis, including acetonitrile and methanol, were of HPLC grade. All the other chemicals and reagents used were of analytical purity grade or higher, and were obtained commercially.

Human hepatoma cells (HepG2) and murine hepatoma cells (H₂₂) were obtained from Shandong Institute of Immunopharmacology and Immunotherapy (Shandong, People's Republic of China). 3-(4,5-Dimethylthiazol-2-yl)-2,5-diphenyltetrazolium bromide (MTT) was purchased from Sigma-Aldrich (St Louis, MO, USA).

Animals

Female Kunming mice (18–22 g) and female Wistar rats (180–220 g) were supplied by Laboratory Animals Center of Shandong University (Shandong, People's Republic

of China). All experiments were carried out in compliance with the requirements of the National Act on the use of experimental animals (People's Republic of China). The experiment was formally approved by an ethics committee, and the protocol number given by the Ethics Committee in Shandong University was 201002050.

HPLC methods to determine TFU and 5-FU concentration

The concentration of TFU was determined at 258 nm by reverse-phase HPLC method (SPD-10Avp pump and LC-10Avp ultraviolet-visible detector; Shimadzu Corporation, Kyoto, Japan). Samples were chromatographed on a 4.6×250 mm reverse-phase stainless steel column packed with 5 µm particles (Venusil XBP C-18; Bonna-Agela China, Tianjin, People's Republic of China) and eluted with a mobile phase (acetonitrile/water, 40:60, v/v) at a flow rate of 1.0 mL/minute. The concentration of 5-FU was detected at 270 nm by reverse-phase HPLC method. The mobile phase for 5-FU measurement was potassium dihydrogen phosphate of 0.1 mol/L with a flow rate of 1.0 mL/minute.

In vitro stability of TFU after incubating with PBS (pH 7.4), simulated gastric fluid, and simulated intestinal fluid

TFU stock solution (acetonitrile/water, 40:60, v/v) was quantitatively diluted with different media, including PBS (0.05 mol/L, pH 7.4), simulated gastric fluid, and simulated intestinal fluid, respectively. Then, the solutions were incubated under horizontal shaking at 37°C±0.5°C. At predetermined time points, 0.5 mL solution was taken out and immersed in an ice bath. After return to room temperature, the samples were immediately filtered through a 0.22 µm Millipore filter. HPLC method was used to determine the content of TFU. Each data point was a mean for the combined data obtained with triplicate samples.

In vitro stability of TFU after incubating with the blank plasma of Wistar rats

Prior to the analysis of TFU in plasma by the HPLC method mentioned above, modified liquid/liquid extraction method was performed. Briefly, 200 µL NaH₂PO₄ solution (0.5 mol/L) and 2 mL ethyl acetate were added in turn into a 200 µL test sample. The mixture was vortexed for 3 minutes and centrifuged at 4,000 rpm for 15 minutes; 1 mL supernatant was transferred into a clean test tube thereafter and evaporated under nitrogen at 50°C–70°C. The residue was

reconstituted with 500 µL mobile phase (acetonitrile/water, 40:60, v/v) and filtered through a 0.22 µm Millipore filter for HPLC determination.²¹

As for 5-FU, 200 µL plasma samples were mixed with 15 µL perchloric acid, followed by vortexing for 3 minutes. The samples were then centrifuged at 15,000 rpm for 10 minutes, and the supernatant was filtered through a 0.22 µm Millipore filter for HPLC determination.

Stock solution of TFU (acetonitrile/water, 40:60, v/v) was quantitatively diluted with blank plasma of Wistar rats. The volume ratio of TFU stock solution to the blank plasma was 1:19. Then, the solution was incubated under horizontal shaking at 37°C±0.5°C. At predetermined time points, a 400 µL sample was taken out and 200 µL was used for TFU determination while the other 200 µL was used for 5-FU determination. Each data point was a mean for the combined data obtained with triplicate samples.

Preparation of TFU-LNS

TFU-LNS were prepared by high-pressure homogenization. Briefly, soya lecithin (5%, w/v) was dispersed in water to obtain an homogeneous dispersion. TFU (0.35%, w/v) powder was poured into the solution and, after a high-speed shearing, the coarse suspensions were obtained. These coarse suspensions were then circulated through the high-pressure homogenizer (NS1001L; GEA Niro Soavi, Parma, Italy) until an equilibrium size was reached. At this point, TFU-LNS were fresh prepared. The fresh-prepared LNS were dispensed into glass vials with mannitol (5%, w/v) as lyoprotectant. The samples were frozen for 24 hours at –80°C then transferred to a freeze-dryer (ALPHA1-2; Martin Christ Gefriertrocknungsanlagen GmbH, Osterode am Harz, Germany) for 48 hours at –40°C at a pressure of 0.5 mbar to get the lyophilized TFU-LNS.

Characterization of TFU-LNS

The morphology of TFU-LNS was examined by transmission electron microscopy (JEM-1200EX; JEOL, Tokyo, Japan). Samples were prepared by placing a drop of TFU-LNS onto a copper grid and air dried, following negative staining with a drop of 2.0% aqueous solution of sodium phosphotungstate for contrast enhancement. The average diameter and zeta potential were determined by laser light scattering (Zetasizer 3000SH; Malvern Instruments, Malvern, UK). The lyophilized TFU-LNS were reconstituted with PBS (pH 7.4) before measurement. Experimental values were calculated from measurements performed at least in triplicate.

Stability of TFU-LNS

To ensure that it would meet clinical needs, the physical stability of the reconstructed TFU-LNS was evaluated at room temperature for 6 hours. The changes in particle size and drug content were recorded.

According to the principles regarding the drug stability in the *Pharmacopoeia of the People's Republic of China*,²² stress testing was carried out. The different lyophilized TFU-LNS were exposed to conditions of high humidity, high illumination, and 40°C temperature for 10 days, respectively.

In addition, different lyophilized TFU-LNS were stored for more than 3 months under sealed conditions at 25°C, 4°C, and -20°C, respectively. The mean particle size and drug content of three groups of TFU-LNS were determined at fixed time intervals.

In vitro release of TFU from TFU-LNS

The in vitro release of TFU from TFU-LNS was conducted using the dialysis bag diffusion technique. Since TFU is insoluble in water, TFU solution (1 mg/mL) in 40% (v/v) mixture of acetonitrile and water was used as control for the in vitro drug release studies.¹ Two milliliters TFU-LNS and TFU solution (final TFU concentration, 1 mg/mL) were each placed into a pre-swelled dialysis bag with 8,000–14,000 Da molecular weight cut-off. Then, the bag was incubated in 100 mL PBS (pH 7.4) at 37°C±0.5°C under horizontal shaking. At predetermined time points, 1 mL samples were taken out and replaced with 1 mL fresh medium. The concentrations of TFU in the samples withdrawn from the incubation medium were analyzed by HPLC as described above. Sink condition was maintained throughout the release period. Data obtained in triplicate were analyzed graphically.

In vitro cytotoxicity

Liver S9 fractions are subcellular fractions that contain drug-metabolizing enzymes, and they are a major tool for studying xenobiotic metabolism. Before the cytotoxicity study, mouse liver S9 fractions were prepared. Kunming mice were sacrificed by decapitation. Livers were quickly removed, rinsed with chilled normal saline (NS), weighed, and minced. The minced livers were homogenized in ice-cold homogenization buffer (50 mM potassium phosphate, 250 mM sucrose, 1 mM ethylenediaminetetraacetic acid, pH 7.4) and centrifuged at 9,000 g for 15 minutes at 4°C. The fat layer was carefully aspirated and the supernatants were the liver S9 fractions. The liver S9 fractions were collected, divided into aliquots, and stored at -80°C until utilized for in vitro assays.^{23,24} The concentration of

the S9 fraction protein (normally 5–20 mg/mL) was analyzed by the Bradford method.²⁵

The in vitro cytotoxicity of TFU-LNS was tested in HepG2 cells using the MTT (thiazolyl blue tetrazolium bromide) assay. The groups were as follows: 1) 5-FU injection; 2) blank LNS; 3) TFU-LNS; 4) TFU-LNS+S9; 5) TFU solution (TFU was dissolved in dimethyl sulfoxide and diluted with cell culture medium); and 6) TFU solution+S9. In groups 4 (TFU-LNS+S9) and 6 (TFU solution+S9), S9 was excessive, and an S9 control group testing was conducted.

Briefly, cells were seeded in 96-well plates at a density of 4,000 viable cells per well and incubated at 37°C in a 5% CO₂ humidified atmosphere overnight to allow cell attachment. Cells were then treated with different doses of test samples in 200 µL of medium at 37°C. After 72 hours of incubation, 20 µL of MTT (5 mg/mL) was added to each well of the plate. After incubating for an additional 4 hours, MTT was aspirated off and 200 µL/well of dimethyl sulfoxide was added to dissolve the formazan crystals. Absorbance was measured at 570 nm and 630 nm with a microplate reader (FL600; Bio-Tek Inc., Winooski, VT, USA). Untreated cells were taken as control with 100% viability and cells without addition of MTT were used as blank to calibrate the spectrophotometer to zero absorbance. In the calculation of the inhibition ratio of group 4 and group 6, the inhibition ratio of S9 was deducted. The results were expressed as mean values ± standard deviation of three measurements.

In vivo antitumor efficacy

The in vivo antitumor efficacy of TFU-LNS was evaluated in H₂₂-bearing Kunming mice after intraperitoneal administration, while an equimolar amount of 5-FU injection was chosen as a control formulation.

H₂₂ cancer cells were extracted from the abdominal dropsy of mice bearing cancer cells and diluted with NS to achieve a cell concentration of 2×10⁷/mL, and 0.1 mL aliquot of cell suspension was subcutaneously injected into mice at the right axillary region.

One day after inoculation, the injected mice were randomly divided into four groups (A–D) with six mice in each group. The mice of group A were injected intraperitoneally with NS as the blank control, and the mice of group B were injected intraperitoneally with blank LNS alone as the carrier control. The mice of Group C were injected intraperitoneally with 5-FU injection (25 mg 5-FU/kg dose) as positive control, and the mice of group D were injected intraperitoneally with TFU-LNS (48 mg TFU/kg dose, equal molar amount of 5-FU

as in group C) as the experimental group. Each group of mice was treated once every other day, five times in total, with their respective formulation.

Tumor volume (V) was calculated by the following formula:

$$V=(W^2 \times L)/2, \quad [1]$$

where W was the smallest superficial diameter of the tumor and L stood for the largest superficial diameter of the tumor. Each animal was weighed just before the time of administration and the dosages were adjusted to maintain the same mg/kg amounts. The weights of each animal were recorded every other day throughout the experiments.

At the end of the experiment (on day 13), the animals were sacrificed and the tumors were harvested, weighed, and photographed. The inhibition rate of tumor weight and tumor volume were calculated according to the following equations, respectively:

$$\text{inhibition rate of tumor weight (\%)} = [(W_c - W_t)/W_c] \times 100; \quad [2]$$

$$\text{inhibition rate of tumor volume (\%)} = [(V_c - V_t)/V_c] \times 100, \quad [3]$$

where W_c and W_t represent the mean tumor weight of control group and treatment group, respectively, while V_c and V_t represent the mean tumor volume of control group and treatment group.

Pharmacokinetics and tissue distribution

The pharmacokinetic properties and tissue distribution of TFU-LNS were investigated in H₂₂-bearing Kunming mice after intravenous administration, comparing to 5-FU injection. The levels of TFU and 5-FU were both measured by the HPLC method in the pharmacokinetic studies as well as in the tissue distribution studies.

Female Kunming mice bearing H₂₂ (100–200 mm³) were randomly assigned to one of two groups and injected intravenously through the tail vein with 5-FU (52 mg 5-FU/kg dose) or TFU-LNS (100 mg TFU/kg dose, equal molar amount of 5-FU as the 5-FU injection group). In each group, blood samples that were taken from the retro-orbital plexus at predetermined time points (0.083, 0.25, 0.5, 0.75, 1, 2, 4, 6, 8, 10, and 12 hours) after drug administration ($n=5$ at each time point) were centrifuged (4,000 rpm, 15 minutes) and plasma were collected and stored. The mice were then sacrificed. The heart, liver, spleen, lung, kidney, tumor, and brain were collected, washed, weighed, and homogenized (ULTRA-TURRAX® homogenizer

[IKS T10]; IKA® Werke GmbH & Co., Staufen, Germany) in 1 mL of NS. TFU and 5-FU were extracted as described above. The amount of TFU and 5-FU in each tissue was determined by the HPLC assay as described above. The data were normalized to the tissue weight.

Pharmacokinetics and statistical analysis

The main pharmacokinetic parameters were calculated using DAS software (v 2.0; Mathematical Pharmacology Professional Committee of China, Shanghai, People's Republic of China). Statistical analysis comparisons between two groups were performed using Student's t -test. $P < 0.05$ was considered significant.

Results

In vitro stability of TFU in different media

As shown in Figure 2, TFU was relatively stable in PBS (pH 7.4) and simulated gastric fluid, while it had a 40% degradation in simulated intestinal fluid. After incubating with the blank plasma of Wistar rats, TFU was almost entirely converted to an equimolar amount of 5-FU within 24 hours.

Characterization of TFU-LNS

The optimized preparation process in this work was as follows: high-speed shearing (3–5 minutes), high-pressure homogenization (200 bar \times five cycles, 500 bar \times ten cycles, 800 bar \times ten cycles, 1,000 bar \times ten cycles). The obtained lyophilized nanosuspensions appeared as white loose powder. The concentration of TFU in fresh TFU-LNS was 3.5 mg/mL, and the drug loading of TFU-LNS was about 6.54%. The lyophilized nanosuspensions showed good redispersibility and the reconstituted nanosuspensions showed light blue opalescence. The TFU-LNS were spherical or ellipsoidal in shape. TFU-LNS had mean particle size of 43.85 ± 1.34 nm and zeta potential of -7.17 ± 1.21 mV, while the lyophilized

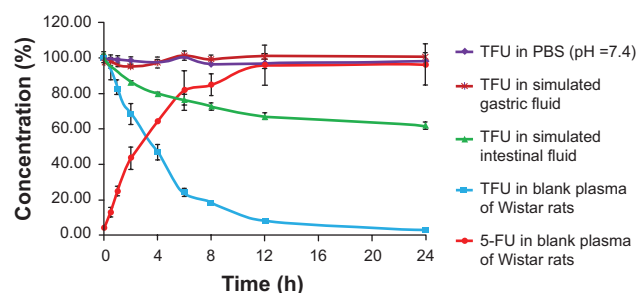


Figure 2 In vitro stability of TFU in different media ($n=3$).

Abbreviations: 5-FU, 5-fluorouracil; PBS, phosphate-buffered saline; TFU, N₃-O-toluyfl-fluorouracil; h, hours.

TFU-LNS had a mean particle size of 180.03 ± 3.11 nm and zeta potential of -8.02 ± 1.43 mV after reconstruction. Three batches of samples showed good reproducibility.

Stability of TFU-LNS

The particle size of TFU-LNS after reconstruction was maintained under 200 nm and the content was almost unchanged at room temperature for 6 hours. This lyophilized powder was sensitive to temperature and illumination, and it was also affected by humidity. The particle size of TFU-LNS grew to 372.30 ± 10.51 nm after 10 days under high-humidity conditions. Either under illumination conditions or at 40°C , yellow shrinkage appeared after 10 days, and the particle size of TFU-LNS grew to 280.23 ± 11.37 nm and 219.90 ± 5.44 nm, respectively. After 3 months, the particle size of TFU-LNS was larger than 200 nm at 25°C or -20°C . It was demonstrated that 4°C was the best storage condition, and, during this storage period, the particle size was not significantly changed and more than 99% of TFU remained in the formulations.

Release of TFU from TFU-LNS in vitro

The in vitro release behavior of TFU from TFU solution (acetonitrile:water = 40:60) could be described by Higuchi equations and expressed by the following equations:

$$Q = 83.49t^{1/2} - 24.88 \quad (r = 0.9920), \quad [4]$$

where t is the release time and Q is the accumulative release percentage. The TFU release behavior from TFU-LNS in vitro was in accordance with bio-exponential kinetics model and expressed by the following equations:

$$100 - Q = 4.655e^{-0.764t} + 2.161e^{-0.093t} \quad (r_\alpha = 0.9975, r_\beta = 0.9905). \quad [5]$$

More than 90% of TFU can be released from the TFU solution within 4 hours, and more than 90% of TFU can be released from TFU-LNS within 4 hours (Figure 3).

In vitro cytotoxicity

The in vitro cytotoxicity of TFU-LNS was assessed by MTT assay in HepG2. The dose required for 50% growth inhibition (IC_{50} value) for the six groups was calculated. The IC_{50} values of 5-FU injection, blank LNS, TFU-LNS, TFU-LNS+S9, TFU solution, and TFU solution+S9 were 57.38 ± 2.98 $\mu\text{mol/L}$, 422.47 ± 42.11 $\mu\text{mol/L}$, 57.10 ± 1.81 $\mu\text{mol/L}$, 17.40 ± 1.41 $\mu\text{mol/L}$, 112.20 ± 6.80 $\mu\text{mol/L}$, and 32.84 ± 0.74 $\mu\text{mol/L}$, respectively. Blank LNS tested as a negative control were observed to be distinctly less toxic than the other five groups. The TFU-LNS and TFU solution were both significantly

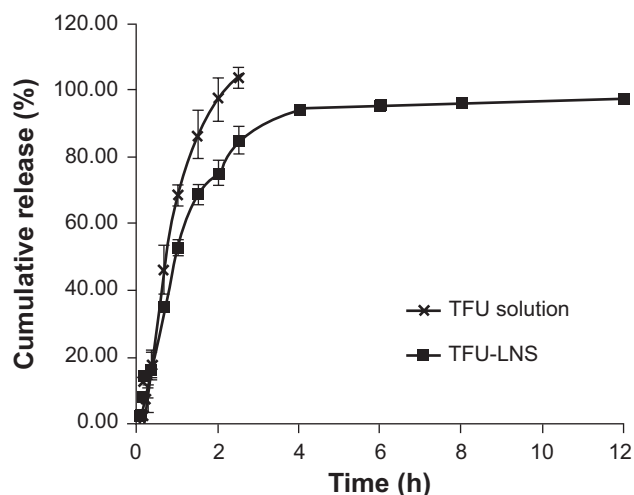


Figure 3 The comparative release curves of TFU solution and TFU-LNS ($n=3$).

Abbreviations: TFU, N_2 -O-toluyyl-fluorouracil; TFU-LNS, TFU-loaded lipid-based nanosuspensions; h, hours.

($P < 0.01$) more effective against hepG2 cells in the presence of liver S9 than TFU-LNS or TFU solution without liver S9. Compared with TFU solution, TFU-LNS revealed more cytotoxicity against HepG2 cells. In addition, the group of TFU-LNS+S9 was more active ($P < 0.01$) than the equal amount of 5-FU injection. The IC_{50} value of blank nanosuspensions was much lower than that of the other five groups.

In vivo antitumor efficacy

Kunming mice implanted with H_{22} cells were used to qualify the relative efficacy of TFU-LNS through intraperitoneal administration. Equal molar amount of 5-FU injection was chosen as the positive control. Figure 4 shows the antitumor effect in each group. The inhibitory rates of tumor weight after administration with TFU-LNS and 5-FU injection were 78.57% and 75.00%, respectively, while the inhibitory rates of tumor volume were 66.67% and 60.00%, respectively (Table 1). No significant difference of inhibitory rate was observed between the group of TFU-LNS and the group of 5-FU injection.

Figure 5 gives the body weight variations of mice in each group during the therapeutic procedure. Compared with the NS group, there was no significant weight loss in mice treated with blank LNS. The results also suggest that the mean body weight of the TFU-LNS group was slightly heavier than that of the 5-FU injection group, which might be explained by the sustained release of 5-FU from TFU-LNS.

Pharmacokinetic studies and biodistribution of TFU-LNS

The concentration in plasma versus time profile of TFU and 5-FU is shown in Figure 6. Table 2 shows the analysis results of the pharmacokinetic statistics with DAS software

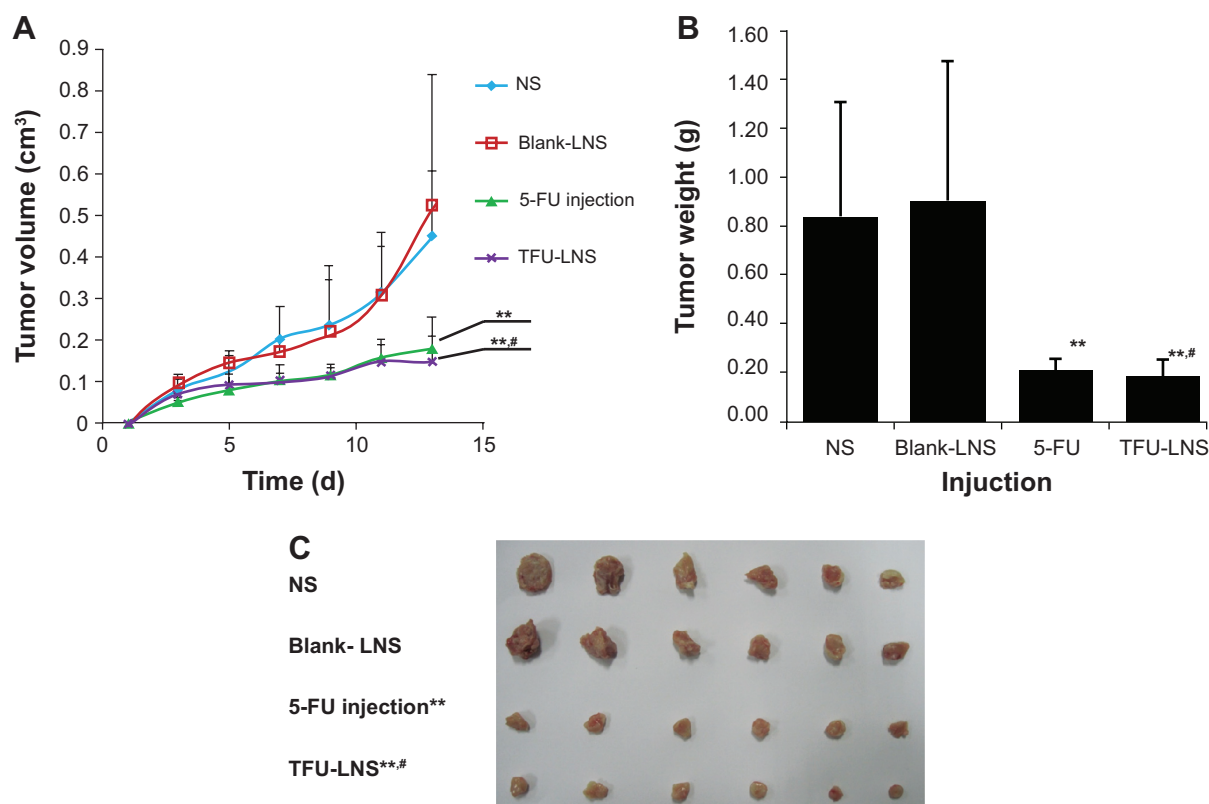


Figure 4 Antitumor effect of TFU-LNS.

Notes: Data represent mean \pm SD (n=6). **(A)** Variation of tumor volume in mice. **(B)** Tumor weight in H₂₂ tumor-bearing mice on day 13. **(C)** Photographs of tumors from each treatment group excised on day 13. ^{**}P<0.01 versus NS; [#]P>0.05 versus 5-FU injection.

Abbreviations: 5-FU, 5-fluorouracil; LNS, lipid-based nanosuspensions; NS, normal saline; SD, standard deviation; TFU-LNS, N₃-O-toluyfl-fluorouracil-loaded LNS; d, days.

(v 2.0). The results of the pharmacokinetic studies in Kunming mice showed that 5-FU could be released from TFU-LNS *in vivo*, and there was no significant difference between the area under the curve of the released 5-FU and that of the injected equal molar amount 5-FU injection. Compared with the 5-FU injection, MRT (mean retention time) and T_{1/2 β} (elimination half-life) of 5-FU released from TFU-LNS increased by about 3.31 and 2.12 times, respectively. It can be seen in Figure 6 that the concentration of 5-FU in the 5-FU injection group reduced quickly, while the release of 5-FU from TFU-LNS was more gradual.

The concentration of TFU and 5-FU versus time in each tissue are shown in Figure 7. Figure 8 shows the area

under the curve (0–8 hours) of TFU and 5-FU in the two groups, which demonstrates that the 5-FU concentrations decreased in both the heart and kidney in the TFU-LNS group. The tumor accumulation amounts of 5-FU in the two groups were almost the same, which was consistent with the results of the pharmacodynamics study. Figure 9 gives the targeting disposition of TFU and 5-FU after intravenous administration of TFU-LNS and 5-FU injection in mice. More than 25% of TFU and 5-FU were detected in the plasma of mice, while the drug content was relatively low in the tissues, indicating the rapid metabolism of TFU and 5-FU *in vivo*.

Table I Inhibitory rate of tumor in H₂₂ tumor-bearing mice (n=6)

Group	Tumor weight (g) \pm SD	Inhibitory rate of tumor weight (%)	Tumor volume (cm ³) \pm SD	Inhibitory rate of tumor volume (%)
NS	0.84 \pm 0.47	NA	0.45 \pm 0.16	NA
Blank LNS	0.90 \pm 0.58	NA	0.52 \pm 0.32	NA
5-FU injection	0.21 \pm 0.05	75.00	0.18 \pm 0.08	60.00
TFU-LNS	0.18 \pm 0.07	78.57	0.15 \pm 0.06	66.67

Note: The data were measured on day 13.

Abbreviations: 5-FU, 5-fluorouracil; LNS, lipid-based nanosuspensions; NS, normal saline; SD, standard deviation; TFU-LNS, N₃-O-toluyfl-fluorouracil-loaded LNS; NA, not available.

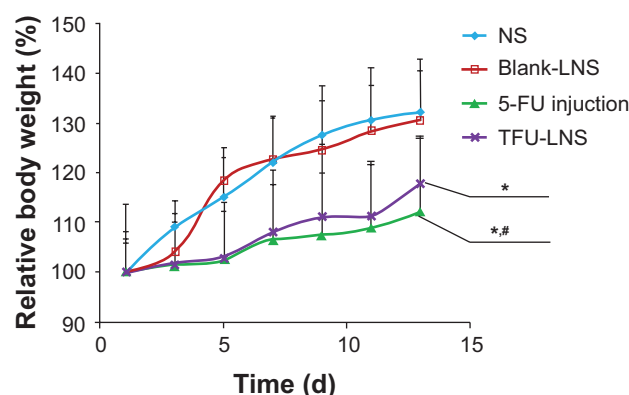


Figure 5 Variation of body weight in H_{22} tumor-bearing mice ($n=6$).

Notes: * $P<0.05$ versus NS; # $P>0.05$ versus 5-FU injection.

Abbreviations: 5-FU, 5-fluorouracil; LNS, lipid-based nanosuspensions; NS, normal saline; TFU-LNS, N_3 -O-toluyfl-fluorouracil-loaded LNS; d, days.

Discussion

TFU was stable in acidic and neutral solution, indicating that TFU could be stable during the preparation process of formulations. TFU was not sensitive to pepsin, but was prone to degrade by trypsin, indicating that TFU might release 5-FU in the intestinal site especially when administered orally. Since TFU was stable both in PBS (pH 7.4) and in simulated gastric fluid (pH 1.2), the degradation in simulated intestinal fluid might be an enzymatic degradation rather than a pH-dependent one. However, whether TFU has intestinal targeting needs further research. Since TFU can be converted to 5-FU gently in plasma in vitro, it can be conjectured that TFU can be transformed into 5-FU in vivo. Therefore, we evaluated the presence of TFU and 5-FU simultaneously in the pharmacokinetic and tissue distribution studies to verify the conjecture on metabolism of TFU-LNS in vivo and provide a theoretical basis for the pharmacodynamics study. Nanosuspension preparation can be broadly classified into two categories: the so-called bottom-up (precipitation) and top-down (media milling,

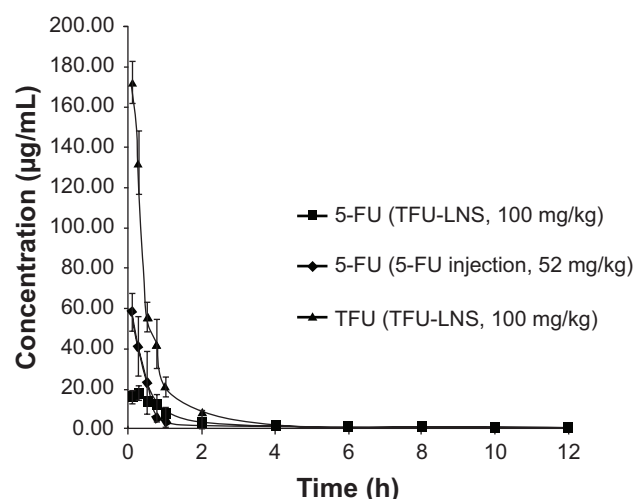


Figure 6 Plasma concentration–time curves of TFU and 5-FU in mice after TFU-LNS (100 mg/kg, equimolar to 5-FU) and 5-FU injection (52 mg/kg) were administrated intravenously ($n=5$).

Abbreviations: 5-FU, 5-fluorouracil; TFU, N_3 -O-toluyfl-fluorouracil; TFU-LNS, TFU-loaded lipid-based nanosuspensions; h, hours.

high-pressure homogenization, etc) types.²⁶ The bottom-up techniques are not widely used because of some prerequisites, such as usage of organic solvents, and the drug should be soluble at least in one solvent.²⁷ The top-down technologies are disintegration methods, which can be employed for all insoluble drugs like TFU.²⁸ In this study, high-pressure homogenization was used for preparing TFU-LNS, which achieved size reduction by the cavitation forces generated when drug dispersion was forced through a very narrow gap under extremely high pressure.^{29,30} The mean particle size of the suspensions was mainly determined by the hardness of the drug, the homogenization pressure, and the number of cycles.³¹ In general, the particle size decreased with an increasing number of cycles and increasing homogenization pressure. However, a good linear relationship could not be obtained between the increase of power consumption and

Table 2 Pharmacokinetic parameters of TFU-LNS and 5-FU injection ($n=5$)

Parameters	TFU-LNS (100 mg/kg)		5-FU injection (52 mg/kg)
	TFU	5-FU	5-FU
AUC _(0–8 h) (mg/L/h)	144.20±10.49	41.34±7.64	45.35±6.04
MRT (h)	2.39±0.80	5.61±2.39*	2.43±1.88
CL (L/h/kg)	0.69±0.05	2.42±0.34	2.21±0.32
T _{1/2α} (h)	0.19±0.02	0.59±0.15**	0.16±0.02
T _{1/2β} (h)	0.75±0.10	0.86±0.23*	0.26±0.16
T _{max} (h)	0.083	0.25**	0.083
C _{max} (mg/L)	172.35±10.70	17.46±3.37**	57.86±9.55

Notes: * $P<0.05$ and ** $P<0.01$ versus 5-FU injection.

Abbreviations: 5-FU, 5-fluorouracil; AUC_(0–8 h), area under the curve (0–8 hours); TFU, N_3 -O-toluyfl-fluorouracil; TFU-LNS, TFU-loaded lipid-based nanosuspensions; h, hours; MRT, mean retention time; CL, clearance; T_{1/2α}, distribution half-life; T_{1/2β}, elimination half-life; T_{max}, time of C_{max}; C_{max}, the peak plasma concentration.

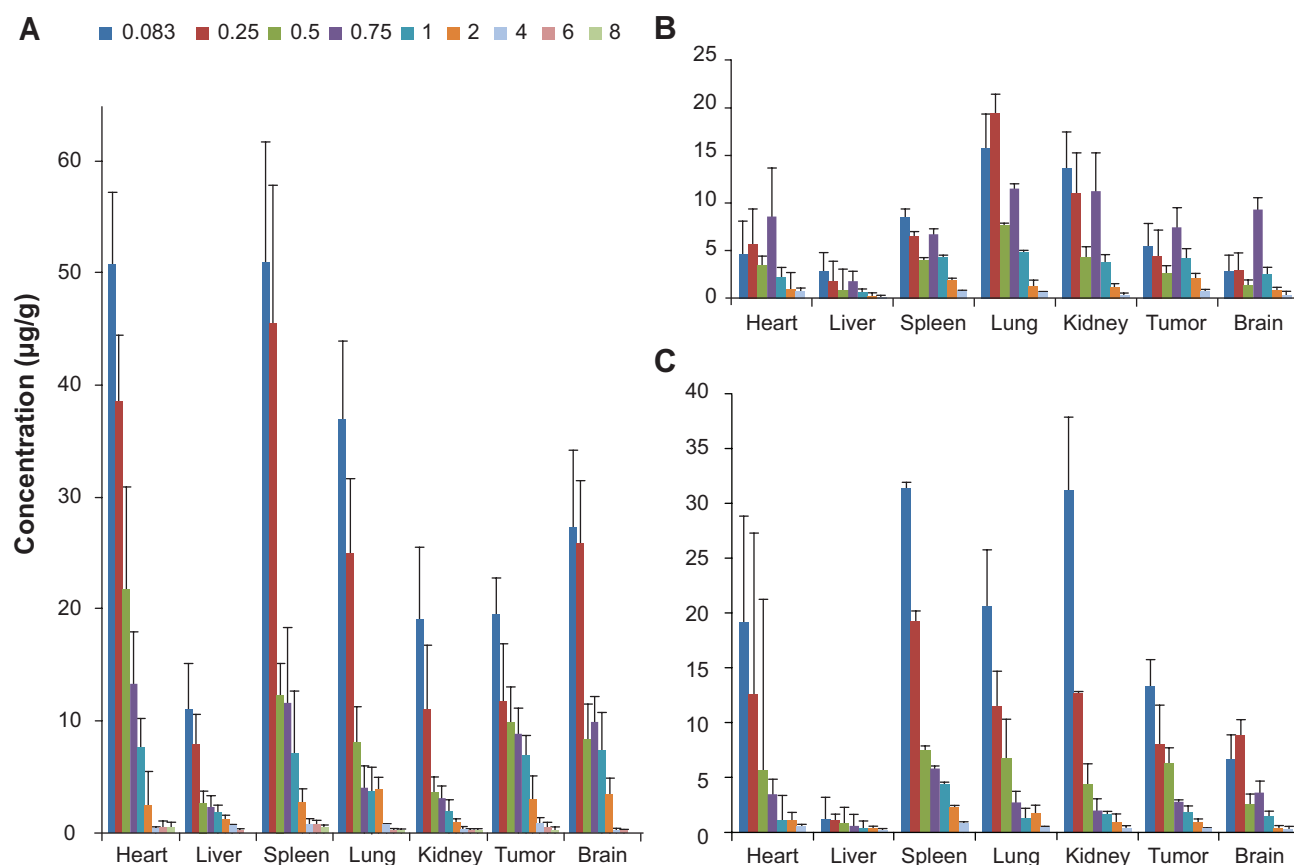


Figure 7 The distribution of TFU and 5-FU at different time points in tumor and each organ.

Notes: (A) The concentration of TFU after administration of TFU-LNS (8.526 mg TFU/mL); (B) the concentration of 5-FU after administration of TFU-LNS; (C) the concentration of 5-FU after administration of 5-FU injection (5.012 mg 5-FU/mL) (n=5).

Abbreviations: 5-FU, 5-fluorouracil; TFU, N₃-O-toluy-fluorouracil; TFU-LNS, TFU-loaded lipid-based nanosuspensions.

the decrease of the particle size. The smaller the particle size was, the more perfect the drug crystals were, and more power consumption was needed. The preparation process was optimized for the best balance of power consumption and product quality. More than 90% of TFU can be released from TFU-LNS within 4 hours, which could be attributed to the improved drug dispersibility.

Stability is one of the critical aspects in ensuring safety and efficacy of drug products. Especially in intravenously administered nanosuspensions, drug particle size and size distribution need to be closely monitored during storage.³² Since phosphatidylcholine is sensitive to temperature and illumination, lyophilization was carried out to improve the stability of TFU-LNS in this work. Further stability studies indicated that TFU-LNS could meet the needs of clinical continuous intravenous infusion after reconstruction, and the lyophilized TFU-LNS had a shelf-life of at least 3 months. It should be noted that the lyophilized TFU-LNS need to be stored at low temperature, in sealed condition, and kept in a dark place.

As 5-FU could not be released from TFU completely without the liver S9 in vitro, the cytotoxicity test showed that TFU solution was less active than the equimolar amount of 5-FU injection. After the liver S9 was added, the IC₅₀ values

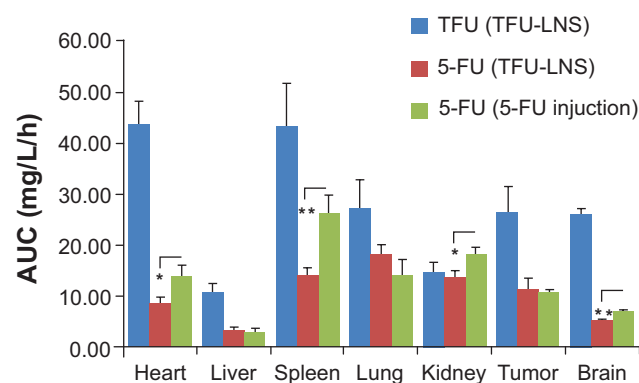


Figure 8 The AUC (0–8 hours) of TFU and 5-FU in tumor and each organ after intravenous administration of TFU-LNS (8.526 mg TFU/mL) and 5-FU injection (5.012 mg 5-FU/mL) (n=5).

Notes: *P<0.05 and **P<0.01 versus 5-FU injection.

Abbreviations: 5-FU, 5-fluorouracil; AUC, area under the curve; TFU, N₃-O-toluy-fluorouracil; TFU-LNS, TFU-loaded lipid-based nanosuspensions; h, hours.

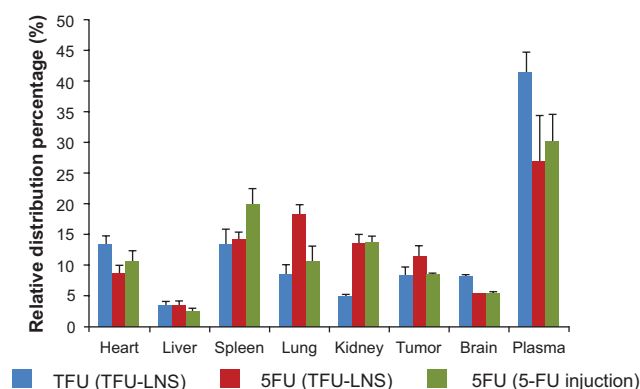


Figure 9 Targeting disposition of TFU and 5-FU in mice after intravenous administration of TFU-LNS (8.526 mg TFU/mL) and 5-FU injection (5.012 mg 5-FU/mL) (n=5).

Abbreviations: 5-FU, 5-fluorouracil; TFU, N₃-O-toluyfl-fluorouracil; TFU-LNS, TFU-loaded lipid-based nanosuspensions.

of TFU-LNS and TFU solution decreased significantly, indicating TFU could be converted into 5-FU and perform antitumor activity. Compared with TFU solution, TFU-LNS revealed higher cytotoxicity against HepG2 cells, which could be explained by the advantages of lipid-based nanocarriers. Phospholipid has been shown to have a good affinity with the cell membrane,^{33,34} which could facilitate cell uptake, enhance the in vitro cytotoxicity, and improve the therapeutic efficacy. Since limited toxicity was observed in the group of the blank LNS, the TFU-LNS were proved to be safe and effective in vitro.

In the antitumor study, TFU-LNS were successfully used in the treatment of H₂₂-bearing Kunming mice after intraperitoneal administration. The inhibitory rates of tumor weight and tumor volume were consistent with those of 5-FU injection. The body weight of mice could be monitored as an index of systemic toxicity. From the variation of body weight in mice, blank LNS had no significant toxicity compared with NS during the therapeutic procedure. One reason was that absolutely no organic solution was added during the preparation of LNS, and another reason was the security of phosphatidylcholine. Phosphatidylcholine is one of the few injectable surfactants that have been used in US Food and Drug Administration-approved pharmaceutical products and have well-established safety profiles and toxicological data.³⁵

After the antitumor study, pharmacokinetic and biodistribution studies were performed. 5-FU could be detected in the blood and each organ of the mice after administration of TFU-LNS. In the group with 5-FU injection, 5-FU was inclined to accumulate in the heart, spleen, and kidney rapidly, and eliminated quickly, while in the TFU-LNS group,

the release of 5-FU from TFU-LNS was slightly slower, and the maximum concentration emerged after 45 minutes in the heart, tumor, and brain, which enhanced the retention time of 5-FU. TFU-LNS had a mean particle size of 180.03±3.11 nm, which were expected to be recognized as foreign matters and be rapidly cleared by phagocytic cells of the mononuclear phagocyte system (MPS), which abound in special tissues and organs, such as liver, lung and spleen.³⁶ However, neither TFU nor 5-FU reached a high level in the liver, which can be explained by the fact that TFU could easily be transformed into 5-FU, and then 5-FU was converted into dihydrofluorouracil to perform antitumor activity due to the existence of enzymes in the liver.³⁷ The tumor accumulation amounts of 5-FU in the two groups verified the results of the pharmacodynamics study quantitatively.

Conclusion

In this study, TFU-LNS were successfully prepared by high-pressure homogenization, which made TFU injectable. In addition, high-pressure homogenization technology provided a relatively easy scale-up opportunity and no organic solvents were added during the preparation. Compared with 5-FU injection, TFU-LNS showed similar antitumor efficacy and better pharmacokinetic properties. Furthermore, this work has been completed as part of a patent application.³⁸ More tumor models that are sensitive to 5-FU, such as human gastric cancer SGC7901 and BGC823 in athymic nude mice, will be examined in future studies. All in all, TFU-LNS may be a promising drug delivery system for cancer therapy.

Acknowledgment

This work was supported by National Key Project on Innovative Drugs (number 2010ZX09401-302-2-29)

Disclosure

The authors report no conflicts of interest in this work.

References

1. Sun W, Zhang N, Li A, Zou W, Xu W. Preparation and evaluation of N(3)-O-toluyfl-fluorouracil-loaded liposomes. *Int J Pharm.* 2008;353(1–2):243–250.
2. Liu J, Li X, Cheng Y, et al. Inhibition of human gastric carcinoma cell growth by treatment of N(3)-o-toluyfl-fluorouracil as a precursor of 5-fluorouracil. *Eur J Pharmacol.* 2007;574(1):1–7.
3. Liu J, Xu WF, Cui SX, et al. Inhibition of human gastric carcinoma cell growth by atofluding derivative N3-o-toluyfl-fluorouracil. *World J Gastroenterol.* 2006;12(42):6766–6770.
4. Zhang X, Zhong JL, Liu W, et al. N(3)-o-toluyfl-fluorouracil inhibits human hepatocellular carcinoma cell growth via sustained release of 5-FU. *Cancer Chemother Pharmacol.* 2010;66(1):11–19.

5. Sun W. *Studies on the TFU-loaded liposomes* [master's thesis]. School of Pharmaceutical Science. Master, Ji'nan: Shandong University; 2007:51–52.
6. Amidon GL, Lennernäs H, Shah VP, Crison JR. A theoretical basis for a biopharmaceutic drug classification: the correlation of in vitro drug product dissolution and in vivo bioavailability. *Pharm Res*. 1995;12(3):413–420.
7. Liu D, Zhang N. Cancer chemotherapy with lipid-based nanocarriers. *Crit Rev Ther Drug Carrier Syst*. 2010;27(5):371–417.
8. Puri A, Loomis K, Smith B, et al. Lipid-based nanoparticles as pharmaceutical drug carriers: from concepts to clinic. *Crit Rev Ther Drug Carrier Syst*. 2009;26(6):523–580.
9. Abdel-Mottaleb M, Neumann D, Lamprecht A. Lipid nanocapsules for dermal application: a comparative study of lipid-based versus polymer-based nanocarriers. *Eur J Pharm Biopharm*. 2011;79(1):36–42.
10. Namiki Y, Fuchigami T, Tada N, et al. Nanomedicine for cancer: lipid-based nanostructures for drug delivery and monitoring. *Acc Chem Res*. 2011;44(10):1080–1093.
11. Lim SB, Banerjee A, Önyüksel H. Improvement of drug safety by the use of lipid-based nanocarriers. *J Control Release*. 2012;163(1):34–45.
12. Zou W, Sun W, Zhang N, Xu W. Enhanced oral bioavailability and absorption mechanism study of N₃-O-toluyyl-fluorouracil-loaded liposomes. *J Biomed Nanotechnol*. 2008;4(1):90–98.
13. Liu D, Liu C, Zou W, Zhang N. Enhanced gastrointestinal absorption of N₃-O-toluyyl-fluorouracil by cationic solid lipid nanoparticles. *J Nanopart Res*. 2010;12(3):975–984.
14. Bai F, Liu C, Dai L, Liu L, Zhang N. [Preparation and pharmacokinetics in mice of N₃-O-toluyyl-fluorouracil solid lipid nanoparticles]. *Chinese Journal of New Drugs and Clinical Remedies*. 2009;28:185–190. Chinese.
15. Liu C, Liu D, Bai F, Zhang J, Zhang N. In vitro and in vivo studies of lipid-based nanocarriers for oral N₃-O-toluyyl-fluorouracil delivery. *Drug Deliv*. 2010;17(5):352–363.
16. Patravale VB, Date AA, Kulkarni RM. Nanosuspensions: a promising drug delivery strategy. *J Pharm Pharmacol*. 2004;56(7):827–840.
17. Verma S, Lan Y, Gokhale R, Burgess DJ. Quality by design approach to understand the process of nanosuspension preparation. *Int J Pharm*. 2009;377(1–2):185–198.
18. Van Eerdenbrugh B, Van den Mooter G, Augustijns P. Top-down production of drug nanocrystals: nanosuspension stabilization, miniaturization and transformation into solid products. *Int J Pharm*. 2008;364(1):64–75.
19. Desai PP, Date AA, Patravale VB. Overcoming poor oral bioavailability using nanoparticle formulations-opportunities and limitations. *Drug Discov Today*. 2012;9(2):87–95.
20. Wang L, Liu Z, Liu D, Liu C, Juan Z, Zhang N. Docetaxel-loaded-lipid-based-nanosuspensions (DTX-LNS): preparation, pharmacokinetics, tissue distribution and antitumor activity. *Int J Pharm*. 2011;413(1–2):194–201.
21. Sun W, Zou W, Huang G, Li A, Zhang N. Pharmacokinetics and targeting property of TFU-loaded liposomes with different sizes after intravenous and oral administration. *J Drug Target*. 2008;16(5):357–365.
22. National Pharmacopoeia Committee. *Pharmacopoeia of the People's Republic of China* [M]. Part 2. Beijing: China Medical Science Press; 2010: Appendix 199–201.
23. Chen J, Halls SC, Alfaro JF, Zhou Z, Hu M. Potential beneficial metabolic interactions between tamoxifen and isoflavones via cytochrome P450-mediated pathways in female rat liver microsomes. *Pharm Res*. 2004;21(11):2095–2104.
24. Tang L, Zhou J, Yang CH, Xia BJ, Hu M, Liu ZQ. Systematic studies of sulfation and glucuronidation of 12 flavonoids in the mouse liver S9 fraction reveals both unique and shared positional preferences. *J Agric Food Chem*. 2012;60(12):3223–3233.
25. Bradford MM. A rapid and sensitive method for the quantitation of microgram quantities of protein utilizing the principle of protein-dye binding. *Anal Biochem*. 1976;72(1–2):248–254.
26. Verma S, Gokhale R, Burgess DJ. A comparative study of top-down and bottom-up approaches for the preparation of micro/nanosuspensions. *Int J Pharm*. 2009;380(1–2):216–222.
27. Gao L, Zhang D, Chen M. Drug nanocrystals for the formulation of poorly soluble drugs and its application as a potential drug delivery system. *J Nanopart Res*. 2008;10(5):845–862.
28. Gao L, Liu G, Ma J, Wang X, Zhou L, Li X. Drug nanocrystals: in vivo performances. *J Control Release*. 2012;160(3):418–430.
29. Sun W, Mao S, Shi Y, Li LC, Fang L. Nanonization of itraconazole by high pressure homogenization: stabilizer optimization and effect of particle size on oral absorption. *J Pharm Sci*. 2011;100(8):3365–3373.
30. Kakran M, Shegokar R, Sahoo NG, Shaal LA, Li L, Müller RH. Fabrication of quercetin nanocrystals: comparison of different methods. *Eur J Pharm Biopharm*. 2012;80(1):113–121.
31. Keck CM, Müller RH. Drug nanocrystals of poorly soluble drugs produced by high pressure homogenisation. *Eur J Pharm Biopharm*. 2006;62(1):3–16.
32. Wu L, Zhang J, Watanabe W. Physical and chemical stability of drug nanoparticles. *Adv Drug Deliv Rev*. 2011;63(6):456–469.
33. Lemmon MA. Membrane recognition by phospholipid-binding domains. *Nat Rev Mol Cell Biol*. 2008;9(2):99–111.
34. van Meer G, Voelker DR, Feigenson GW. Membrane lipids: where they are and how they behave. *Nat Rev Mol Cell Biol*. 2008;9(2):112–124.
35. Koo OM, Rubinstein I, Onyüksel H. Role of nanotechnology in targeted drug delivery and imaging: a concise review. *Nanomedicine*. 2005;1(3):193–212.
36. Gao L, Zhang D, Chen M, et al. Studies on pharmacokinetics and tissue distribution of oridonin nanosuspensions. *Int J Pharm*. 2008;355(1–2):321–327.
37. Stevens AN, Morris PG, Iles RA, Sheldon PW, Griffiths JR. 5-fluorouracil metabolism monitored in vivo by 19F NMR. *Br J Cancer*. 1984;50(1):113–117.
38. Zhang N, Zhang J, Xu W, Liu Y, Wang L, inventors. N₃-O-toluyyl-fluorouracil-loaded nanosuspension and its lyophilized formulation. China patent 201110393143.X. 2012 June 13.

International Journal of Nanomedicine

Publish your work in this journal

The International Journal of Nanomedicine is an international, peer-reviewed journal focusing on the application of nanotechnology in diagnostics, therapeutics, and drug delivery systems throughout the biomedical field. This journal is indexed on PubMed Central, MedLine, CAS, SciSearch®, Current Contents®/Clinical Medicine,

Submit your manuscript here: <http://www.dovepress.com/international-journal-of-nanomedicine-journal>

Dovepress

Journal Citation Reports/Science Edition, EMBASE, Scopus and the Elsevier Bibliographic databases. The manuscript management system is completely online and includes a very quick and fair peer-review system, which is all easy to use. Visit <http://www.dovepress.com/testimonials.php> to read real quotes from published authors.